Fish and Shellfish Immunology 86 (2019) 393–402

Contents lists available at ScienceDirect

Fish and Shellfish Immunology

journal homepage: www.elsevier.com/locate/fsi

Full length article

Identification and functional characterization of grass carp (*Ctenopharyngodon idella*) tumor necrosis factor receptor 2 and its soluble form with potentiality for targeting inflammation

Shengnan Zhang, Xinyan Wang, Chenglong Li, Shiyu Feng, Anying Zhang, Kun Yang, Hong Zhou*

School of Life Science and Technology, Center for Informational Biology, University of Electronic Science and Technology of China, Chengdu, PR China

ARTICLE INFO

Keywords:
Tnf-α receptor 2
Soluble form
Functional identification
Bacterial infection
Anti-inflammation
Grass carp

ABSTRACT

Tumor necrosis factor-alpha (TNF-α) signals through two distinct cell surface receptors, TNFR1 and TNFR2 in mammals. In the present study, grass carp Tnfr2 (gcTnfr2) was isolated and characterized. Sequence alignment and phylogenetic analysis suggested that gcTnfr2 was a homolog of goldfish and zebrafish Tnfr2. Tissue distribution assay showed *gctnfr2* transcripts were expressed in all examined tissues similar to *gctnfr1*. To functionally characterize the newly cloned molecule, gcTnfr2 was overexpressed in COS7 cell lines and it showed the ability to mediate the recombinant grass carp Tnf (rgcTnf)-α-triggered NF-κB activity and *gcil1b* promoter activity, clarifying its role in mediating Tnf-α signaling. The recombinant soluble form of gcTnfr2 (rgcsTnfr2) was prepared and it was able to interact with rgcTnf-α with higher affinity than that of rgcsTnfr1. Moreover, grass carp soluble Tnfr2 (gcsTnfr2) were detected in the culture medium of grass carp head kidney leukocytes (HKLs) and heat-inactivated *A. hydrophila* challenge significantly induced its production, indicating involvement of gcsTnfr2 in inflammation response. In agreement with this notion, rgcsTnfr2 effectively antagonized the effect of rgcTnf-α on *il1b* mRNA expression in HKLs, suggesting anti-Tnf-α property of gcsTnfr2. To strengthen the anti-inflammatory role of soluble Tnfr2, bacteria were injected intraperitoneally in grass carp followed by rgcsTnfr2. Hematoxylin-eosin (HE) staining of head kidney, spleen and intestine showed that rgcsTnfr2 could significantly improve infection-induced histopathological changes. These results functionally identified gcTnfr2 and its soluble form, particularly highlighting the role of gcsTnfr2 against Tnf-α-triggered inflammatory signaling. In this line, rgcsTnfr2 displayed anti-inflammatory potentiality during infection, thereby providing a powerful mediator of inflammation control in fish.

1. Introduction

Tumor necrosis factor-α (TNF-α) is a curial mediator of inflammatory response and immunity, as well as apoptosis [1–5]. The bioactivities of TNF-α are mediated by two distinct cell surface receptors, TNF-α receptor 1 (TNFR1) and 2 (TNFR2). TNFR1 is ubiquitously expressed in almost all cell types [6,7], while TNFR2 is a 75 kDa protein and mainly found in immune cells such as T cells [8,9] and thymocytes [7,10], as well as in endothelial cells [11] and neurological cells, such as TNF-α and IL-1-stimulated astrocytes [12]. Actually, not only does TNFR1 attract extensive attention [6,13], but also there are plenty of reports about TNFR2 signal pathway [14–16]. Generally, TNF binding to trimeric TNFR2 leads to the direct interaction with TNF receptor-associated factors 2 (TRAF2), and then recruits TRAF1, TRAF3, cellular inhibitor of apoptosis protein-1 (cIAP1) and cIAP2 [14,17]. Consequently, NF-κB pathway is activated, leading to transcriptional activation of the genes related to proliferation and survival [2,14,18]. In some studies, TNFR2 triggers the degradation of TRAF2 and terminates the intracellular signal under certain conditions [16,17]. Interestingly, TNFR2 activation can result in cell death in some cells although it lacks death domain in the intracellular region [19–21]. In addition, TNFR2 activation induces the depletion of TRAF2 and accelerates TNFR1-dependent activation of caspase-8, implying the crosstalk between two receptors [3,22,23]. Notably, these two receptors can be cleaved by the cell membrane-anchored proteinase TNF-α converting enzyme (TACE), resulting in soluble TNFR1 and TNFR2 production in serum [24]. Importantly, soluble TNFR1 and TNFR2 retain biological activity and their circulating forms contribute to inflammation, stress response, and development of cardiovascular disease and cancer, thereby implying their clinical roles [17,25,26].

* Corresponding author. School of Life Science and Technology, University of Electronic Science and Technology of China, Chengdu, 610054, PR China.
E-mail address: zhouhongzh@uestc.edu.cn (H. Zhou).

https://doi.org/10.1016/j.fsi.2018.11.061
Received 12 August 2018; Received in revised form 15 October 2018; Accepted 27 November 2018
Available online 28 November 2018
1050-4648/

To date, Tnf-α receptor (Tnfr) 2 has been identified only in Japanese flounder (*Paralichthys olivaceus*) [27] and goldfish (*Carassius aurutus*) [28]. Similar to the low homology of Tnfr1 in fish and mammals, flounder Tnfr2 shares only 33% amino acid identity to its human homolog. Multiple alignment of goldfish Tnfr2 with other known Tnfr2 protein sequences suggests that it shares high homology with the predicted zebrafish Tnfr2 [28]. Therefore, functional characterization of Tnfr2 in fish is indispensable. In addition, as potent biomarkers for immune responses in mammals [17], whether soluble Tnf-α receptors are produced and possess similar activity in fish still remain unknown.

In our previous study, we have identified grass carp Tnfr1 (gcTnfr1) and demonstrated its involvement in Tnf-α signaling [29]. Given that Tnfr2 is another receptor for Tnf-α, we cloned *tnfr2* cDNA from grass carp (*gctnfr2*) and analyzed its expression patterns in various tissues. Further functional analysis revealed that gcTnfr2 could mediate rgcTnf-α signaling. In particular, grass carp soluble Tnfr2 (gcsTnfr2) were detected in the supernatant of grass carp head kidney leukocytes (HKLs) culture and its release were induced by heat-inactivated *A. hydrophila*, indicating its involvement in inflammatory response. Accordingly, the recombinant soluble gcTnfr2 (rgcsTnfr2) was prepared and it showed anti-inflammatory activities against both rgcTnf-α-triggered signaling in HKLs and *in vivo* infection-induced histopathological alternations. We functionally characterized soluble Tnfr in fish for the first time and provided a potential mediator to control fish inflammation.

2. Materials and methods

2.1. Fish

Healthy Chinese grass carp weighting about 1.0 kg were purchased from Chengdu Tongwei Aquatic Science and Technology Company (Chengdu, China). The fish were kept in aerated tap water at 20 ± 2 °C and acclimatized in the laboratory for two weeks before experiments as reported previously [30]. The fish were fed daily with dry food from Tongwei Aquatic Science and Technology Company. All experiments complied with the Regulation of Animal Use in Sichuan Province, China, and were approved by the ethics committee of the University of Electronic Science and Technology of China.

2.2. Cloning and sequencing of gctnfr2 cDNA

Total RNA was extracted from trunk kidney of grass carp by using Tripure Isolation Reagent (Roche, Basel, Switzerland) and the first strand cDNA was synthesized using the M-MLV Reverse Transcriptase system (Promega, WI, USA) according to the manufacturer's protocol. The partial sequence of *gctnfr2* was obtained by PCR using High Fidelity Taq (NEB, Beijing, China) and primers of *tnfr2-F* and *tnfr2-R* (Supplementary Table 1), designed based on the conserved regions of *tnfr2* sequences in other fishes. According to the partial sequence of *gctnfr2*, the 5′- and 3′-RACE were performed to obtain the cDNA sequence of *gctnfr2* with gene-specific primers in Supplementary Table 1. Finally, the full-length cDNA sequence of *gctnfr2* was amplified by High Fidelity Taq (NEB) and sequenced.

2.3. In silico analysis of gcTnfr2

Homology analysis of *gctnfr2* was performed using the BLAST program (https://blast.ncbi.nlm.nih.gov/Blast.cgi) in the National Center for Biotechnology Information (NCBI). The amino acid sequence of gcTnfr2 was deduced using Translate tool in the ExPASy Molecular Biology server (http://web.expasy.org/translate/). Theoretical isoelectric point (pI) and molecular weight (MW) of deduced gcTnfr2 protein were calculated by Compute pI/MW in Expert Protein Analysis System (http://expasy.org/tools/). Signal peptide was predicted using the SignalP 4.1 (http://www.cbs.dtu.dk/services/SignalP/). The domains and motifs of gcTnfr2 were analyzed by SMART program (http://smart.embl-heidelberg.de/) and protein BLAST in NCBI. Multiple sequence alignment was created with DNAMAN and phylogenetic tree of TNFR2 homologs was developed using MEGA 4.

2.4. Tissue distribution of gctnfr2 transcripts

Total RNA was extracted from different organs including spleen, thymus, liver, heart, gill, intestine, brain, and head kidney of healthy grass carp by using Tripure Isolation Reagent (Roche). Total RNA was reverse-transcribed to cDNAs independently as described above and used as templates to quantitate the expression levels of *gctnfr2* and *bactin* by real-time PCR (RT-qPCR). RT-qPCR was performed on a Bio-Rad CFX96 Real-time detection system (Bio-Rad, Hercules, USA) in a final volume of 20 μL containing 10 μL of Real Master Mix (Tiangen, Beijing, China), 2 μL of the cDNA, and 0.5 μL of forward and reverse gene specific primers (10 μM) (Supplementary Table 1). A standard curve was generated for each target molecule by using the 10-fold serial dilutions (from 10^{-1} to 10^{-6} fmol) of plasmid containing the target gene sequence as template to evaluate the amplification efficiency. In these experiments, each group contained four samples and *bactin* was amplified as the internal control.

2.5. Construction of gcTnfr2 expression plasmids

The *gctnfr2* open reading frame was cloned using the Phusion High-Fidelity DNA Polymerase (Thermo Fisher Scientific, Waltham, USA) and primers with restriction endonuclease recognition sites (Supplementary Table 1) were designed based on the cDNA sequence of *gctnfr2*. The cloned PCR products were sequenced as described above and then digested by using the corresponding restriction endonuclease. After that, the digested PCR fragments encoding *gctnfr2* were inserted into pCMV5-Flag to obtain gcTnfr2 expression vector (pCMV5-Flag-*gctnfr2*). The integrity of inserted DNA was verified by sequencing and the plasmids were extracted by using a TIAN prep Mini Plasmid Kit (Tiangen) for later use.

2.6. Cell culture and transfection

COS7 cells (Center for Type Culture Collection, Wuhan, China) (1.8×10^5 cells/well) were seeded in 24-well plates (Corning, NY, USA) with 500 μL/well Opti-MEM medium (Gibco, NY, USA) or at 8×10^5 cells per well in a 6-well plate (Corning) with 1500 μL/well Opti-MEM medium (Gibco) and incubated at 37 °C overnight. The transfection assay was performed as described preciously [31,32]. Briefly, COS7 cells in 6-well plate were incubated with the mixture containing 2 μg of pCMV5-Flag-*gctnfr2* plasmid or empty vector (pCMV5-Flag) and 1.5 μL of Lipofectamine 2000 (Invitrogen) for 6 h. And cells were collected 48 h after transfection to determine whether gcTnfr2 was overexpressed. Western blotting assay was used to detect the overexpressed gcTnfr2 with an anti-Flag antibody (1:2000, Cell Signaling Technology, MA, USA) as described in our previous study [31]. Subsequently, COS7 cells in a 24-well plate were transfected with the mixture containing 400 ng of pGL6-pNF-κB-luc (Beyotime biotechnology, Shanghai, China) that carries four tandem copies of the NF-κB binding consensus sequence (GGGAATTTCC) fused to a pTA promoter, or pGL3-p*gcil-1β*-luc which was constructed by inserting gcIl-1β promoter region into pGL3 basic vector (Promega) as described previously [29] and 300 ng of pCMV5-Flag-*gctnfr2* or pCMV5-Flag, 10 ng of pRL-TK Vector (Promega, WI, USA) and 1.5 μL of Lipofectamine 2000 (Invitrogen) for 6 h. After 24 h transfection, the cells were treated with recombinant grass carp Tnf-α (rgcTnf-α) (200 ng/mL) prepared as described previously [33] for 12 h. Subsequently, the cells were lysed by 100 μL of Passive Lysis Buffer (Promega) and the luciferase activities were detected by using a Dual-Luciferase Reporter Assay System (Promega) as described previously [32].

2.7. Recombinant expression of extracellular region of gcTnfr2

The cDNA fragment encoding the extracellular region of *gctnfr2* (from position 64 to 789) was amplified by the Phusion High-Fidelity DNA Polymerase (Thermo Fisher Scientific) and the gene specific primers with restriction endonuclease recognition sites (*rgctnfr2pE-F-BamH* I and *rgctnfr2pE-R-Xhol I*, Supplementary Table 1). The PCR products and the pET30a (+) expression vector (Novagen, Darmstadt, Germany) were digested by the endonucleases: BamH I and Xhol I (NEB) and they were ligated by T4 ligase (Promega). The integrity of inserted DNA was verified by sequencing. The plasmids (pET30a-rgcsTnfr2) were extracted by using a TIAN prep Mini Plasmid Kit (Tiangen) and transformed into *Escherichia coli* BL21 (DE3). The positive colony was cultured in LB broth with 25 μg/mL kanamycin at 37 °C to OD_{600nm} of 0.6–0.8. The inducer, IPTG (Merck, Darmstadt, Germany), with concentration of 1 mM was used to induce the recombinant protein expression at 30 °C. After induction for 6 h, the bacteria were collected by centrifugation at 4 °C and sonicated on ice. The target protein (nominated as rgcsTnfr2) was purified using HisTrap affinity columns (GE Healthcare, Waukesha, USA) and desalted by Superdex25 per grade columns (GE Healthcare). The molecular weight and purity of recombinant proteins were analyzed on SDS-PAGE and identified by Western blotting using an anti-His antibody (1:600, Boster, Wuhan, China). Bradford method was used to measure the concentration of target protein. The purified rgcsTnfr2 protein was lyophilized and then stored at −80 °C for further use.

2.8. Western blotting (WB) assay of soluble gcTnfr2 in HKLs

Grass carp HKLs were isolated using a discontinuous density gradient centrifugation as reported previously [30,33]. In brief, head kidney was isolated from grass carp under sterile conditions and gently squeezed to release the cells into the medium. After filtrated through 200 μm nylon mesh, the leukocytes were separated by density gradient centrifugation (Ficoll-Hypaque 1.083 kg/L, TBD, Tianjin, China) at 400 × *g* for 30 min at 20 °C. Leukocytes at the interface were collected and washed twice using washing buffer. Then cells were resuspended in RPMI-1640 medium supplemented with 10% fetal bovine serum (Gibco) and seeded in 35 mm dish (Corning) at the density of 1×10^7 cells/well. Finally, the cells were incubated at 28 °C under 5% CO_2 and saturated humidity. In the following day, HKLs were challenged with heated-inactivated pathogenic bacteria strain of *Aeromonashydrophila subsp. hydrophila* (*A. hydrophila*), which has been described previously [31,34] at concentration of 1×10^7 CFU/dish for 1 h or 3 h. Subsequently, the supernatant of culture medium was collected and concentrated by ultrafiltration. In this assay, the gcTnfr2 polyclonal antibodies (anti-gcTnfr2 pAb) were the custom product of the company of Biogot (Nanjing, China). To validate its specificity, recombinant gcsTnfr2 and the concentrated culture medium of HKLs were analyzed by WB in which the membrane was incubated with anti-gcTnfr2 pAb or the antibody pre-absorbed with 10 μg of rgcsTnfr2. The proteins in culture medium were separated by SDS-PAGE gel and WB assay was used to detect soluble gcTnfr2 with anti-gcTnfr2 pAb (1:5000). In parallel, β-actin in HKL lysates was detected as a control by using a monoclonal antibody for β-actin (1:5000, ZSGB-BIO, Beijing, China).

2.9. Binding of extracellular region of gcTnfr1 and gcTnfr2 with rgcTnf-α

Since rgcsTnfr1 was obtained in our previous study [29], *in vitro* binding of rgcsTnfr1 and rgcsTnfr2 with rgcTnf-α was compared by quantitative ELISA as described in our previous studies [29,33]. In brief, rgcsTnfr2, rgcsTnfr1 or BSA (negative control) with increasing amounts (from 0 to 20 pmol/well) was coated in a 96-well polystyrene plate (Costar, MA, USA) for 16 h at 4 °C. In the next day, the coated wells were blocked with blocking buffer (0.3% BSA and 5% nonfat milk in PBS) for 4 h at room temperature. After the wells washed for 3 times, 20 pmol of rgcTnf-α was added to each well and incubated for 2 h. Subsequently, the wells were washed with PBST (0.05% Tween-20 in PBS) for four times and 100 μL of HRP conjugated rgcTnf-α Ab (1:1000) was added into each well. The samples were incubated for 2 h at room temperature. After washing for five times, 100 μL of substrate (1 mg/mL, 3,3′,5,5′-Tetramethylbenzidine, Tiangen) was added into each well and the samples were incubated for 30 min at 37 °C. Finally, 2 M H_2SO_4 was added to terminate reactions and the OD values at 450 nm were determined by a Bio-Rad iMark Microlpate Reader (Bio-Rad).

2.10. Expression analysis of grass carp il1b mRNA in HKLs

Grass carp HKLs were isolated using a discontinuous density gradient centrifugation as described in section 2.8. The isolated cells (6×10^5 cells/well) were seeded in 24-well plate (Corning) and incubated at 28 °C under 5% CO_2 and saturated humidity. On the following day, HKLs were challenged with rgcTnf-α (200 ng/mL) in the absence or presence of rgcsTnfr2 (107 ng/mL, the molar ratio of rgcTnf-α and rgcsTnfr2 was 2:1). Three hours later, the cells were collected, and total RNA was extracted. The mRNA levels of *gcil1b* and *bactin* were assayed by RT-qPCR as described above.

2.11. Hematoxylin-eosin (HE) staining of grass carp tissues

Before *A. hydrophila* infection, healthy grass carp with body weight about 60 g were fed in laboratory for two weeks and then transferred into four tanks (5 fish/tank) containing 1000 L clean water. The bacteria were cultured in 100 mL TSB medium at 28 °C with shaking at 180 rpm for 18 h. Subsequently, *A. hydrophila* were collected and resuspended in PBS (pH 7.4) and spread on a TSA plate to determine the amount of *A. hydrophila*. In the four tanks, two groups of fish were injected intraperitoneally (i.p.) with rgcsTnfr2 (0.1 mL/fish, 10 μg/fish) and sterilized PBS (0.1 mL/fish), respectively, and the other two groups were received i.p. injections with the bacteria (0.1 mL/fish; 1×10^8 CFU/mL in PBS) 30 min prior to treatment with or without rgcsTnfr2 (10 μg/fish). After that, tissues (head kidney, spleen and intestine) were isolated at 1-day post-infection from different groups and HE staining was performed. Briefly, tissue samples from four groups (PBS group, rgcsTnfr2 group, infection group and rgcsTnfr2 group following infection) were fixed in 4% neutral buffered paraformaldehyde (Sigma-Aldrich, MO, USA) for 24 h and dehydrated in ascending concentrations of alcohol and cleaned in xylol. These tissues were embedded in paraffin and sectioned with a rotary microtome. The tissue slices were stained with hematoxylin and eosin and the stained sections were visualized by using the BX51 system (OLYMPUS, Tokyo, Japan).

2.12. Data analysis

Statistical analysis was conducted using one-way analysis of variance (ANOVA) followed by Fisher's least significant difference (LSD) tests using SPSS13.0 software. For comparison between two groups, Student's *t*-test was used. Significant difference and highly significant difference were considered at $p < 0.05$ and $p < 0.01$, respectively.

3. Results

3.1. Isolation and sequence analysis of gctnfr2

The full-length cDNA sequence of *gctnfr2* (GenBank ID: MH674091) contained 70 bp of 5′-UTR, 185 bp of 3′-UTR and the ORF of 1335 bp encoding 444 amino acids (aa). Two mRNA instability motifs (ATTTA) followed by a polyA tail were found in 3′-UTR (Supplementary Fig. 1). Nucleotide BLAST of *gctnfr2* in NCBI showed *gctnfr2* was a member of TNFR superfamily. The putative gcTnfr2 protein had a predicted signal peptide of 20 aa and the mature peptide of 45.76 kDa with a pI of 6.37. Alignment of amino acid sequences revealed gcTnfr2 shared relatively

Table 1
Amino acid and nucleotide identities of grass carp Tnfr2 compared with the known TNFR2 sequences in other species. All identities are expressed as a score ratio. The italicized numerals stand for amino acid identities.

Identity (%)	1	2	3	4	5	6	7	8	9
1 Grass carp		65.85	74.01	38.61	32.29	32.40	34.11	30.45	31.4
2 Zebrafish	*55.13*		63.51	36.08	33.17	34.34	31.00	30.22	32.88
3 Goldfish	*60.57*	*51.08*		38.06	29.95	31.36	32.21	30.59	33.33
4 Flounder	*28.23*	*24.31*	*24.85*		25.80	32.92	34.37	35.89	32.88
5 Chicken	*22.2*	*22.15*	*18.91*	*23.03*		41.44	35.84	34.53	36.64
6 Cattle	*23.43*	*22.20*	*22.40*	*21.14*	*30.10*		83.98	64.02	76.73
7 Pig	*23.33*	*23.34*	*18.13*	*21.29*	*30.74*	*80.04*		66.53	78.46
8 Mouse	*21.68*	*20.17*	*22.29*	*23.63*	*27.95*	*55.72*	*58.92*		*70.29*
9 Human	*23.17*	*22.04*	*23.30*	*21.57*	*28.08*	*69.10*	*72.44*	*60.67*	

low identities (21.41%–22.74%) with its mammalian counterparts, and higher homology with goldfish and zebrafish homologs (62.77% and 56.25%, respectively) (Table 1). Like other TNFR superfamily members, gcTnfr2 possessed a 243 aa of extracellular domain, a 23 aa of transmembrane region and a 158 aa of intracellular domain (Fig. 1A). The gcTnfr2 extracellular domain possessed four cysteine rich domains (CRDs) compared with three CRDs in gcTnfr1 [29]. Furthermore, in the cytoplasmic region of gcTnfr2, three predicted Traf2 binding sites were found, which are presumably significant for Tnf-Tnfr2 signal pathway. It is different from gcTnfr1 that there is no death domain in the intracellular region of gcTnfr2. Similar to gcTnfr1 [29], gcTnfr2 contained four predicted N-glycosylated sites. Unrooted phylogenetic tree was constructed to confirm the close evolutionary relationship of gcTnfr2 with goldfish and zebrafish Tnfr2. As shown in Fig. 1B, all Tnfr1s and Tnfr2s were clustered into two branches, the fish Tnfr2 branched together and separated from mammalian Tnfr2 clade. Meanwhile, gcTnfr2 was grouped closely to goldfish Tnfr2.

3.2. Analysis of *gctnfr2* transcripts in healthy grass carp tissues

RT-qPCR was used to detect the expression pattern of *gctnfr2* in various tissues of grass carp. As shown in Fig. 2, *gctnfr2* mRNA was ubiquitously expressed in all selected tissues. The transcripts of *gctnfr2* were most abundantly in intestine, heart and head kidney, relatively low levels in spleen, thymus, liver, and brain. The lowest expression level of *gctnfr2* was found in gill.

3.3. Effects of gcTnfr2 overexpression on NF-κB activity and *gcil-1β* promoter activity in COS7 cells

To clarify whether gcTnfr2 mediates gcTnf-α signaling, transfection of gcTnfr2 was performed in COS7 cells, and the overexpressed gcTnfr2 was confirmed by WB assay. As shown in Fig. 3A, a band of approximately 51 kDa, which was the size of gcTnfr2 linked flag fusion protein, was found in the cell lysates. Besides, another band of 75 kDa with high level was also detected, possibly being the glycosylated form of gcTnfr2. By contrast, there was no band detected in empty plasmids-transfected cell lysates (Fig. 3A). Subsequent luciferase activity assay was performed and revealed that overexpression of gcTnfr2 was effective in enhancing rgcTnf-α-induced NF-κB activity, as well as *gcil-1β* promoter activity (Fig. 3B and C).

3.4. Production and purification of rgcsTnfr2

The rgcsTnfr2 was produced in the supernatant of the crude protein extraction of IPTG-induced *Escherichia coli BL21 (DE3)* cells and purified by Ni-NTA metal affinity chromatography. SDS-PAGE analysis revealed that the purified proteins showed a major band with 33 kDa and a slight band of 66 kDa which were the same size as the gcsTnfr2 monomer and homodimer, respectively (Fig. 4A). Besides, His-tag mAb could recognize these two protein bands as shown in Fig. 4B.

3.5. Determination of soluble gcTnfr2 in grass carp HKLs

To demonstrate the existence of soluble gcTnfr2, the culture medium of grass carp HKLs was collected and WB assay was performed. In this case, the specificity of anti-gcTnfr2 pAb was validated, showing that it could specifically recognize monomeric rgcsTnfr2 with a size of about 33 kDa (Fig. 5A, line 1) and a single band with the size of about 26 kDa from the culture medium (Fig. 5A, line 2). The latter one is corresponding to the predicted MW of natural gcsTnfr2. Nevertheless, in the antibody pre-absorption experiment, the binds for both rgcsTnfr2 and natural gcsTnfr2 were not observed (Fig. 5B). Subsequently, the gcsTnfr2 with 26 kDa could be detected in the culture medium of grass carp HKLs in the presence and absence of *A. hydrophila* challenge (Fig. 5C). Moreover, *A. hydrophila* markedly enhanced the production of gcsTnfr2 at 1 h but not 3 h (Fig. 5C).

3.6. Binding analysis of rgcsTnfr1 and rgcsTnfr2 with rgcTnf-α

To investigate the interaction of rgcsTnfr2 with rgcTnf-α, the direct *in vitro* binding assay base on quantitative ELISA was performed as described in previous studies [29,34]. As shown in Fig. 6A, rgcsTnfr2 (0–20 pmol/well) displayed the binding ability to rgcTnf-α in a dose-dependent manner and it reached to saturation when the concentration of rgcTnf-α and rgcsTnfr2 were 20 pmol and 15 pmol, respectively. The binding was not found expectedly in the control group with increasing amounts of BSA. In parallel, the affinity of rgcsTnfr2 binding to rgcTnf-α was obviously higher than that of rgcsTnfr1.

3.7. Antagonistic effect of rgcsTnfr2 on rgcTnf-α-induced responses in HKLs

To assess the role of rgcsTnfr2 in mediating rgcTnf-α responses, grass carp HKLs were treated with rgcTnf-α (150 ng/mL) in the presence or absence of rgcsTnfr2 (107 ng/mL, the rgcTnf-α mixed with rgcsTnfr2 at molar ratio 2:1) and the levels of *gcil1b* mRNA regulated by rgcTnf-α was detected. As shown in Fig. 6B, rgcTnf-α could stimulate the *gcil1b* mRNA expression and this stimulation was blocked by rgcsTnfr2. Additionally, rgcsTnfr2 and heat-inactivated rgcsTnfr2 was unable to change basal *gcil1b* mRNA expression (Fig. 6B).

3.8. Evaluation of rgcsTnfr2 antagonism against A. hydrophila infection in vivo

To assess the anti-inflammatory role of rgcsTnfr2, it was injected i.p. into *A. hydrophila* pre-infected grass carp. HE staining showed that tissues (head kidney, intestine and spleen) in control group displayed normal structures (Figs. 7A, 8A and 9A). In the intestine from PBS-treated fish, a continuous thin submucous layer under muscular layer was observed (Fig. 8A). Moreover, no signs of damage, hemorrhage and inflammation were found in three tissues (Figs. 7A, 8A and 9A). Compared with control groups, rgcsTnfr2 did not cause considerable pathological changes or hemorrhage in three tissue samples (Figs. 7B, 8B

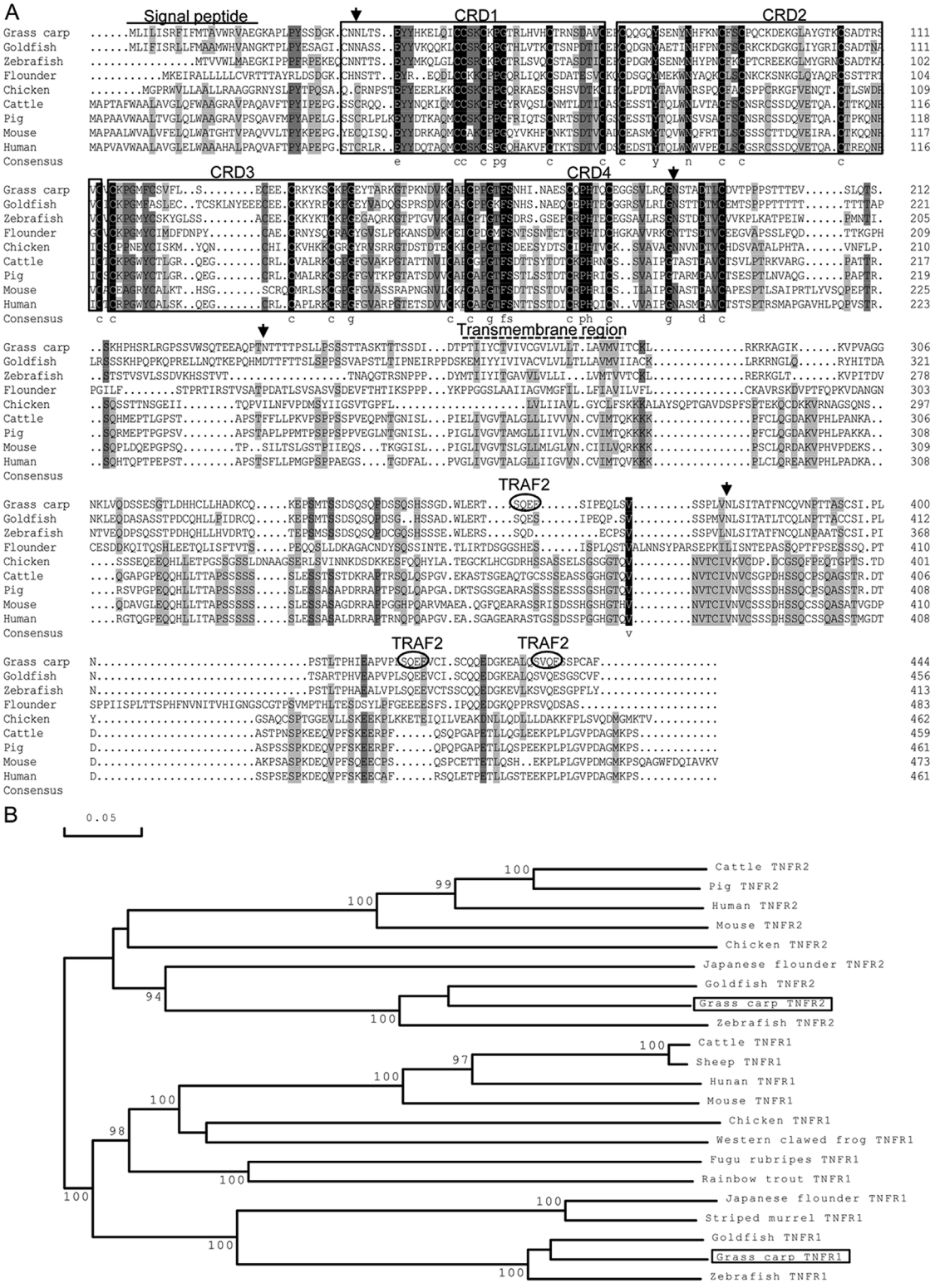

Fig. 1. (A) Amino acid alignment of gcTnfr2 with the known Tnfr2 homologs in other vertebrates. The putative signal peptide sequence is marked by an overhead line. Cysteine rich domains (CRDs) are showed with black boxes and the lowercases under the boxes indicated the fully conserved amino acid residues. The dot-dashed line indicates the transmembrane region and the predicted N-glycosylated sites are labeled by black arrows above the sequence. The predicted TRAF2 binding sites are displayed with black ellipses. (B) An unrooted phylogenetic tree is constructed by the neighbor joining method using amino acid sequences of Tnfr1 and Tnfr2 in various vertebrates and the numbers indicate the bootstrap confidence values obtained for each node after 1000 replications. The scale on the bottom refers to the percentage divergence (p-distance). Grass carp Tnfr1 and Tnfr2 were displayed with black line rectangle. GenBank accession numbers of Tnfr1 and Tnfr2 protein in this analysis: Human TNFR1: P19438; Mouse TNFR1: P25118; Pig TNFR1: P50555; Cattle TNFR1: O19131; Chicken TNFR1: NP_001025950; Clawed frog TNFR1: BAF95748; Fugu rubripes Tnfr1: XP_011604193; Rainbow trout Tnfr1: CCG34104; Zebrafish Tnfr1: NP_571915; Goldfish Tnfr1: ACR08664; Japanese flounder Tnfr1: BAC65225; Snakehead murrel Tnfr1: CCQ71731; Grass carp Tnfr1: KX094934; Human TNFR2: NP_001057; Mouse TNFR2: NP_035740; Pig TNFR2: NP_001090910; Cattle TNFR2: NP_00035580; Chicken TNFR2: NP_989770; Japanese flounder Tnfr2: AB080947; Goldfish Tnfr2: FJ905477; Zebrafish Tnfr2: XP_001336489; Grass carp Tnfr2: MH674091.

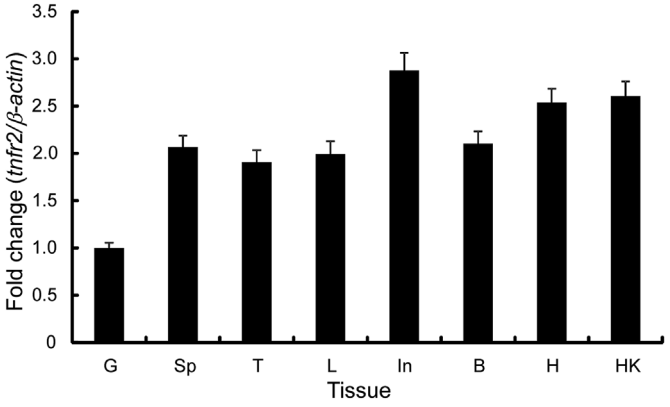

Fig. 2. Quantitative analysis of *gctnfr2* mRNA expression in various tissues of grass carp. The RT-qPCR was performed using the primers specific for *gctnfr2* or *bactin*. The *gctnfr2* expression was relative to endogenous control gene *bactin* in the same sample and all results were normalized against *gctnfr2* mRNA level in gill. Sp: spleen; T: thymus; Li: liver; H: heart; G: gill; In: intestine; B: brain; HK: head kidney. Data presented are expressed as mean ± SEM ($N = 3$).

and 9B). However, bacterial infection resulted in an increase of vacuole, serious hemorrhage and inflammatory cell infiltration in head kidney (Fig. 7C). Not unexpectedly, these symptoms induced by bacterial challenge were remarkably reduced by rgcsTnfr2 injection (Fig. 7D). Similarly, the increase of vacuole and hemorrhage were also observed in intestine and spleen after bacteria infection compared with those in control groups (Figs. 8C and 9C), and these symptoms of inflammation were improved by rgcsTnfr2 injection (Figs. 8D and 9D). Moreover, other pathological symptoms of the bacterial infected-intestine were observed, including erythrocytes and inflammatory cell infiltration in the submucous layer, and the increase of submucous layer thickness and hemorrhage in the lumen of villus (Fig. 8C), but rgcsTnfr2 could significantly reduce these histopathological changes (Fig. 8D).

4. Discussion

Here, we obtained the cDNA sequence of *gctnfr2*, and structure analysis revealed that gcTnfr2 shared the conserved signature motifs of TNFRSF (CRD) and possessed similar domains with goldfish and Japanese flounder Tnfr2 (Supplementary Fig. 1) but was lack of death domain as mammalian TNFR2 [35]. Similar to mammalian TNFR2, all fish Tnfr2s contained four CRDs in the ectodomain of receptors (Fig. 1A), which is different from fish Tnfr1 with three CRDs [28,29]. In higher vertebrates, the first CRD is conducted to the formation of homotrimer, the second and third CRDs are involved in ligand binding activity and the last one is related to ligand-receptor dissociation [36,37]. Further phylogenetic tree based on amino acid sequences support gcTnfr2 as the ortholog of mammalian TNFR2. Notably, alignment analysis revealed that gcTnfr2 shared relatively low amino acid identities with its homologs in other species as seen in gcTnfr1 [29], and functional characterization is required to define gcTnfr2 as a member of Tnfr family.

It is known that NF-κB signal pathway was activated by both TNFR1 and TNFR2 [17,38], we detected NF-κB activity in COS7 cells with the overexpressed gcTnfr2, showing that the overexpression of gcTnfr2 could mediate rgcTnf-α-triggered NF-κB activity (Fig. 3B). Given that NF-κB is well known as a global activator of numerous pro-inflammatory cytokines and chemokines and to play a critical role in modulating activation and function of immune system [39,40], our results imply the importance of Tnf-α-Tnfr2 signaling in fish inflammatory regulation. In our data, overexpression of gcTnfr2 affected rgcTnf-α-induced *gcil-1β* promoter activity (Fig. 3C). Taken these data together, not only the function of gcTnfr2 mediating gcTnf-α signaling was demonstrated, but also its role in the induction of inflammation as gcTnfr1 was established [29].

In mammals, it is generally accepted that the soluble TNF receptors are formed by the cleavage of the extracellular region of TNFR1 and TNFR2 [24]. In this line, the soluble TNFR1 and TNFR2 are found in circulating bloods, and their serum levels may correlate the course and outcome of some diseases and cancer [17,26,41–43], indicating their clinical significance. However, whether soluble Tnfr is produced and released in fish remains unclear. In this study, we detected the soluble Tnfr2 in the culture medium of grass carp HKLs, providing evidence for the existence of soluble Tnfr as in mammals. Moreover, a rapid and marked increase of soluble Tnfr2 levels caused by heat-inactivated *A. hydrophila* challenge was observed in the same cell model (Fig. 5C), implying its involvement in inflammation regulation.

To investigate the role of soluble Tnfr2, rgcsTnfr2 was prepared and

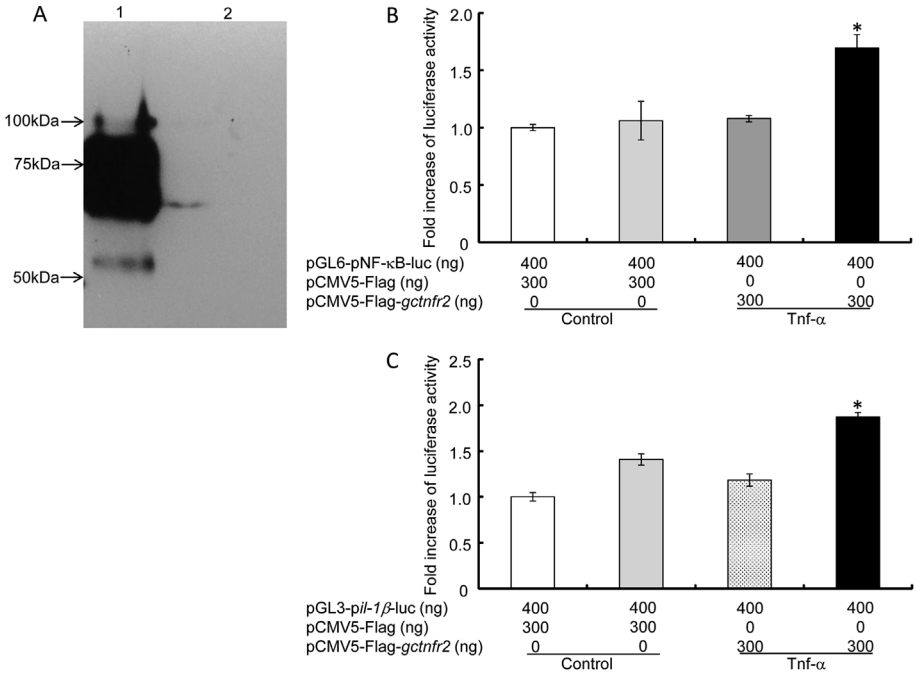

Fig. 3. Functional identification of gcTnfr2 in mediating gcTnf-α signaling. (A) Overexpression of gcTnfr2 in COS7 cells. COS7 cells were transfected with the pCMV5-Flag-gcTnfr2 plasmid or empty vector (pCMV5-Flag) for 48 h. Western blotting confirmed the overexpression of gcTnfr2 by using anti-Flag antibody (1:2000). (B) NF-κB activity was monitored by a pGL6-pNF-κB-TA-Luc reporter system in COS7 cells co-transfected with pCMV5-Flag-gcTnfr2 or empty vectors (pCMV5-Flag) in the presence or absence of rgcTnf-α (200 ng/mL). The cells were collected, and the luciferase activity was measured and renilla luciferase activity was used as internal control. (C) Similar assay was performed to examine *gcil-1β* promoter activity by using pGL3-p*gcil-1β*-TA-Luc reporter system. Data presented are expressed as mean ± SEM ($N = 4$). The asterisk (*) represents significant differences at $p < 0.05$ vs. the control.

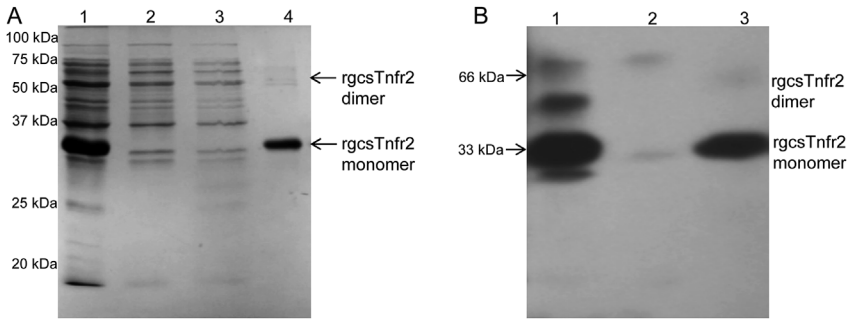

Fig. 4. Purification of rgcsTnfr2. (A) SDS-PAGE analysis of rgcsTnfr2. Lane 1: Total protein before purification; lane 2: The protein of flow through; lane 3: The protein eluted by 20 mM imidazole; lane 4: The purified protein. (B) Verification of the purified rgcsTnfr2 by Western blotting analysis using anti-His antibody (1:600). Lane 1: Total protein before purification; lane 2: The protein of flow through; lane 3: The purified protein of rgcsTnfr2.

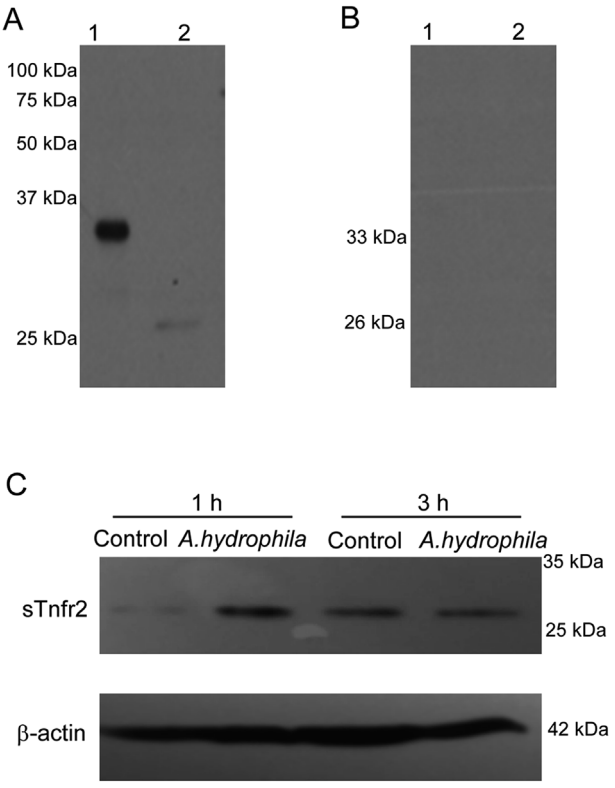

Fig. 5. The determination of soluble gcTnfr2 in grass carp HKLs. (A) The specificity of anti-gcTnfr2 pAb was validated by Western blotting. Lane 1: rgcsTnfr2; lane 2: The culture medium of grass carp HKLs. (B) Western blotting analysis of rgcsTnfr2 and culture medium of grass carp HKLs using anti-gcTnfr2 pAb pre-absorbed with 10 μg of rgcsTnfr2. Lane 1: rgcsTnfr2; lane 2: The culture medium of grass carp HKLs. (C) Effects of *A. hydrophila* treatment on gcsTnfr2 in grass carp HKLs. HKLs were seeded in 35 mm dish with density of 1×10^7/dish and incubated at 28 °C under 5% CO_2 and saturated humidity. After the cells were challenged with or without heated-inactivated *A. hydrophila* at concentration of 1×10^7 CFU/dish for 1 h or 3 h, the medium of each dish was collected and concentrated by ultrafiltration. The culture medium and cell lysates were analyzed by Western blotting assay using anti-gcTnfr2 pAb (1:5000) and β-actin mAb (1:5000), respectively.

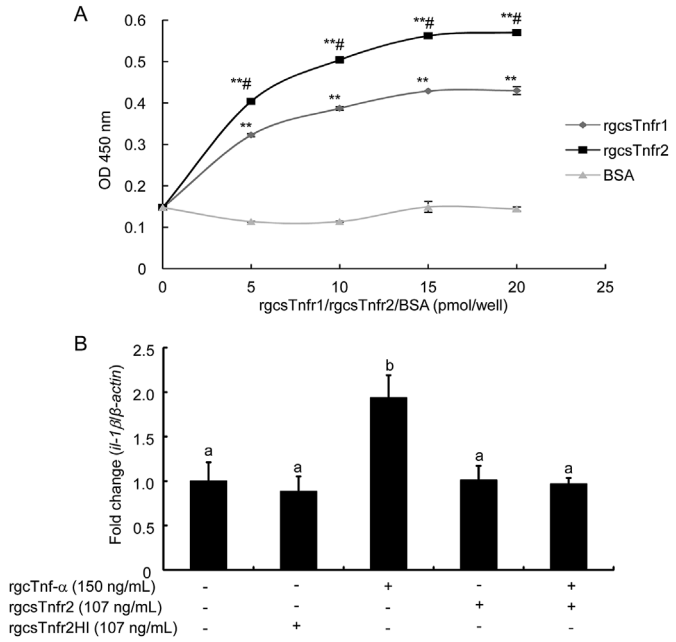

Fig. 6. Interaction between rgcsTnfr1 or rgcsTnfr2 and rgcTnf-α *in vitro*. (A) The binding of rgcsTnfr1 or rgcsTnfr2 with rgcTnf-α. The 96-well plates were coated with different amounts (from 0 to 20 pmol/well) of rgcsTnfr1, rgcsTnfr2 or BSA (control) at 4 °C overnight. Then the pre-coated wells were incubated with rgcTnf-α (20 pmol/well) after washing and blocking. The binding was detected by using anti-gcTnf-α antibody conjugated HRP. Data presented are expressed as mean ± SEM ($N = 3$). The asterisk (**) denotes highly significant difference at $p < 0.01$ (vs. BSA control) and the hash symbol (#) indicated the significant difference at $p < 0.01$ between rgcsTnfr1 and rgcsTnfr2 groups. (B) Antagonistic effect of rgcsTnfr2 on rgcTnf-α response in grass carp HKLs. Cells were treated with rgcsTnfr2 (107 ng/mL), rgcTnf-α (200 ng/mL) or rgcTnf-α (200 ng/mL) in combination of rgcsTnfr2 (107 ng/mL). The rgcTnf-α-treated group was served as positive control and the group without drug treatment was served as negative control. Three hours later, *gcil1b* mRNA levels were detected by RT-qPCR and analyzed using an internal control *bactin* and expressed as fold changes of the control group. Data presented are expressed as mean ± SEM ($N = 4$). The alphabet denotes a significant difference at $p < 0.05$ vs. the control group.

purified. Similar to recombinant expression proteins of goldfish Tnfr and rgcsTnfr1 [28,29], rgcsTnfr2 had both monomeric and homodimeric forms (Fig. 4A and B). In agreement with this, recombinant Tnf-α proteins of various fish species all have homodimeric forms as mentioned in our previous study [44]. This indicates that Tnf-α and its receptors are inclined to dimerization in fish. Interestingly, binding assay found that rgcsTnfr2 bound to rgcTnf-α specifically in a dose-dependent manner and its affinity with rgcTnf-α was stronger than that of rgcsTnfr1 (Fig. 6A), which was consistent with the findings that the affinity of TNFR2 for TNF-α is greater than that of TNFR1 in mammals [1,2]. Accordingly, soluble Tnfr2 might mediate an immune response by interacting with TNF-α. To address this hypothesis, the effect of rgcsTnfr2 on rgcTnf-α response was examined in HKLs, showing that rgcsTnfr2 significantly attenuated rgcTnf-α-induced *il1b* mRNA expression (Fig. 6B). Additionally, rgcsTnfr1, and recombinant extracellular proteins of goldfish Tnfr1 and Tnfr2 also display the ability to abrogate Tnf-α-primed inflammatory responses in immune cells [28,29]. The antagonism of the extracellular domain of fish Tnfr supported the notion that soluble receptors may play important role to limit Tnf-α-triggered inflammatory signaling in fish.

In clinical application, anti-TNF therapies are widely used in inflammatory disease and the development of anti-TNF agents is of great

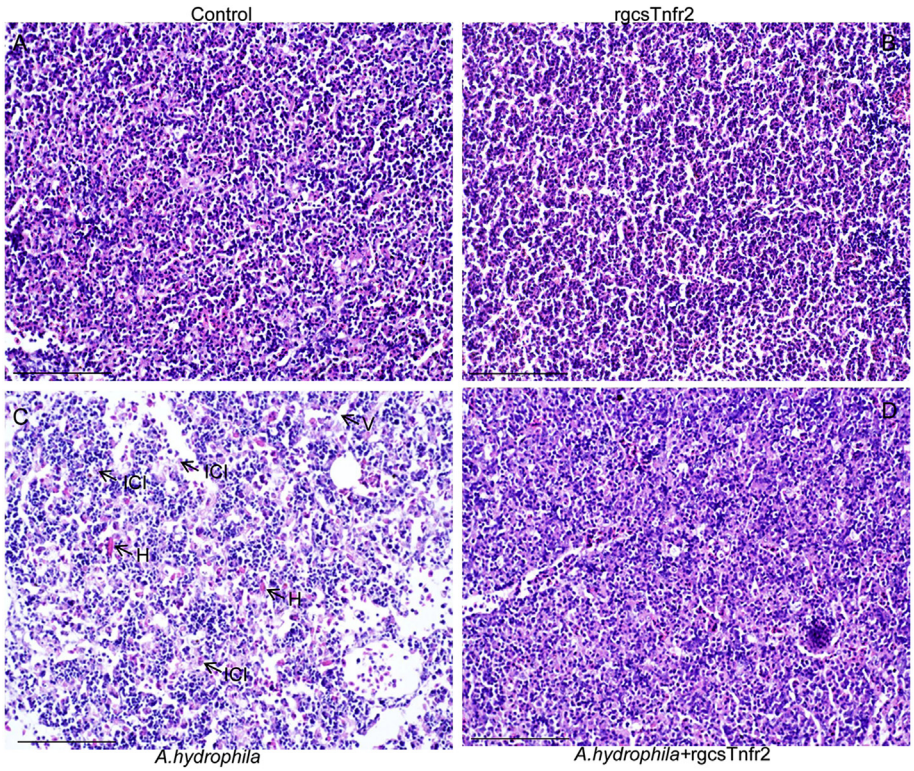

Fig. 7. The representative photos of the histological alterations in head kidney at 1-day post-infection (magnification, × 400; scale bar, 200 μm). (A) PBS group. (B) rgcsTnfr2 group. (C) *A. hydrophila* infection group. (D) rgcsTnfr2 injection group followed by *A. hydrophila* infection. V, Vacuole. H, Hemorrhage. ICI, Inflammatory cell infiltration.

interest, particular production of anti-TNF antibodies and recombinant proteins of soluble TNFR [45,46]. Considering the higher affinity of TNFR2 to TNF-α than that of TNFR1, recombinant proteins of soluble TNFR2 is thought as a potent TNF-α antagonist for the treatment of inflammation [47]. It has been reported that the *A. hydrophila* infection leads to histopathological change in grass carp [48]. In this regard, rgcsTnfr2 was used to treat grass carp infected by *A. hydrophila*, and HE staining assay revealed that the rgcsTnfr2 treatment show an anti-inflammatory effect in spleen, intestine and head kidney, suggesting the therapeutic potential of rgcsTnfr2.

Conclusively, our results functionally characterized gcTnfr2, particularly highlighting the existence and anti-inflammatory role of gcsTnfr2. These findings will help to understand the functional role of Tnfr2 in fish immunity and lay the foundation for the development of

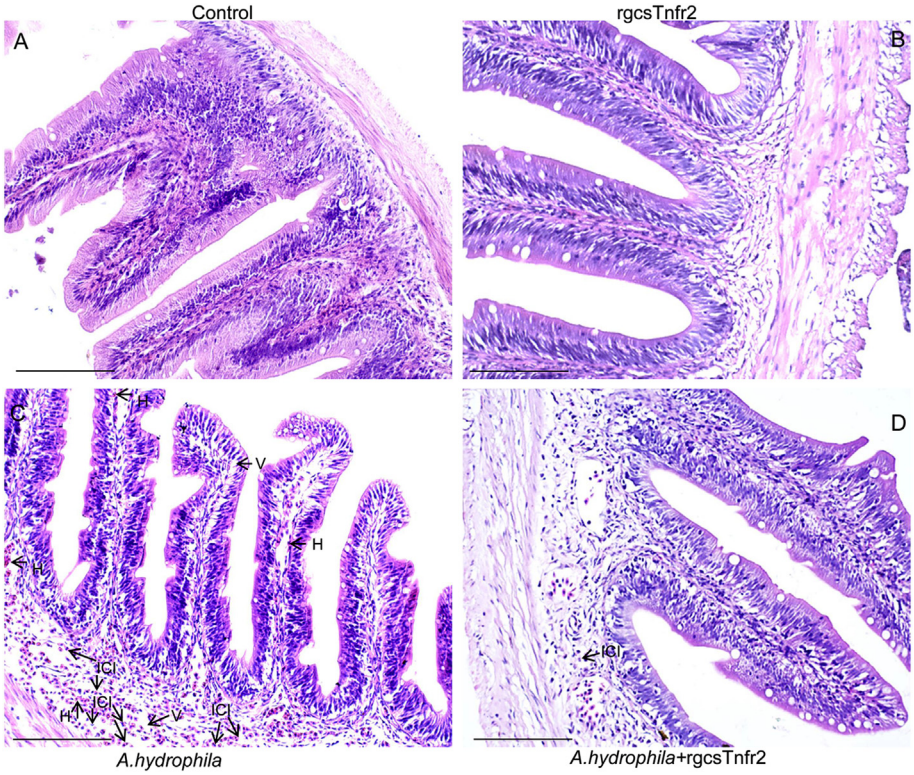

Fig. 8. The representative photos of the histological changes in intestine at 1-day post-infection (magnification, × 400; scale bar, 200 μm). (A) PBS group. (B) rgcsTnfr2 group. (C) *A. hydrophila* infection group. (D) rgcsTnfr2 injection group followed by *A. hydrophila* infection. V, Vacuole. H, Hemorrhage. ICI, Inflammatory cell infiltration.

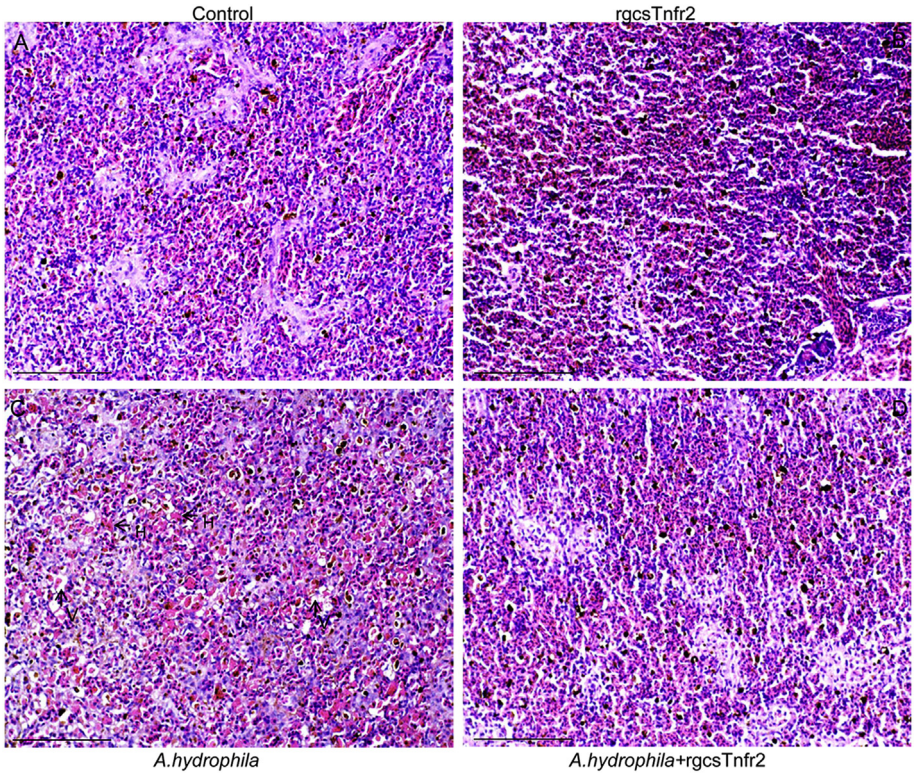

Fig. 9. The representative photos of the histological alterations in spleen at 1-day post-infection (magnification, × 400; scale bar, 200 μm). (A) PBS group. (B) rgcsTnfr2 group. (C) *A. hydrophila* infection group. (D) rgcsTnfr2 injection group followed by *A. hydrophila* infection. V, Vacuole. H, Hemorrhage.

anti-inflammatory agents in teleost.

Acknowledgements

This work was supported by the grants from the National Natural Science Foundation of China, China (31572650, 31471181).

Appendix A. Supplementary data

Supplementary data to this article can be found online at https://doi.org/10.1016/j.fsi.2018.11.061.

References

[1] R.M. Locksley, N. Killeen, M.J. Lenardo, The TNF and TNF receptor superfamilies: integrating mammalian biology, Cell 104 (2001) 487–501.
[2] D.J. MacEwan, TNF ligands and receptors–a matter of life and death, Br. J. Pharmacol. 135 (2002) 855–875.
[3] M. Fotin-Mleczek, F. Henkler, D. Samel, M. Reichwein, A. Hausser, I. Parmryd, P. Scheurich, J.A. Schmid, H. Wajant, Apoptotic crosstalk of TNF receptors: TNF-R2-induces depletion of TRAF2 and IAP proteins and accelerates TNF-R1-dependent activation of caspase-8, J. Cell Sci. 115 (2002) 2757–2770.
[4] B.B. Aggarwal, Tumour necrosis factors receptor associated signalling molecules and their role in activation of apoptosis, JNK and NF-kappaB, Ann. Rheum. Dis. 59 (Suppl 1) (2000) i6–16.
[5] L. Wang, F. Du, X. Wang, TNF-alpha induces two distinct caspase-8 activation pathways, Cell 133 (2008) 693–703.
[6] G. Chen, D.V. Goeddel, TNF-R1 signaling: a beautiful pathway, Science 296 (2002) 1634–1635.
[7] M. Grell, E. Douni, H. Wajant, M. Lohden, M. Clauss, B. Maxeiner, S. Georgopoulos, W. Lesslauer, G. Kollias, K. Pfizenmaier, P. Scheurich, The transmembrane form of tumor necrosis factor is the prime activating ligand of the 80 kDa tumor necrosis factor receptor, Cell 83 (1995) 793–802.
[8] L.A. Tartaglia, R.F. Weber, I.S. Figari, C. Reynolds, M.A. Palladino Jr., D.V. Goeddel, The two different receptors for tumor necrosis factor mediate distinct cellular responses, Proc. Natl. Acad. Sci. U. S. A. 88 (1991) 9292–9296.
[9] H.P. Hohmann, R. Remy, M. Brockhaus, A.P. van Loon, Two different cell types have different major receptors for human tumor necrosis factor (TNF alpha), J. Biol. Chem. 264 (1989) 14927–14934.
[10] M. Grell, F.M. Becke, H. Wajant, D.N. Mannel, P. Scheurich, TNF receptor type 2 mediates thymocyte proliferation independently of TNF receptor type 1, Eur. J. Immunol. 28 (1998) 257–263.
[11] S. Bertok, M.R. Wilson, A.D. Dorr, J.O. Dokpesi, K.P. O'Dea, N. Marczin, M. Takata, Characterization of TNF receptor subtype expression and signaling on pulmonary endothelial cells in mice, Am. J. Physiol. Lung Cell Mol. Physiol. 300 (2011) L781–L789.
[12] S.J. Choi, K.H. Lee, H.S. Park, S.K. Kim, C.M. Koh, J.Y. Park, Differential expression, shedding, cytokine regulation and function of TNFR1 and TNFR2 in human fetal astrocytes, Yonsei Med. J. 46 (2005) 818–826.
[13] W.M. Chu, Tumor necrosis factor, Cancer Lett. 328 (2013) 222–225.
[14] V. Baud, M. Karin, Signal transduction by tumor necrosis factor and its relatives, Trends Cell Biol. 11 (2001) 372–377.
[15] Z. Chen, T.D. Palmer, Differential roles of TNFR1 and TNFR2 signaling in adult hippocampal neurogenesis, Brain Behav. Immun. 30 (2013) 45–53.
[16] M. Rodriguez, L. Cabal-Hierro, M.T. Carcedo, J.M. Iglesias, N. Artime, B.G. Darnay, P.S. Lazo, NF-kappaB signal triggering and termination by tumor necrosis factor receptor 2, J. Biol. Chem. 286 (2011) 22814–22824.
[17] L. Cabal-Hierro, P.S. Lazo, Signal transduction by tumor necrosis factor receptors, Cell. Signal. 24 (2012) 1297–1305.
[18] N.J. Maney, G. Reynolds, A. Krippner-Heidenreich, C.M.U. Hilkens, Dendritic cell maturation and survival are differentially regulated by TNFR1 and TNFR2, J. Immunol. 193 (2014) 4914–4923.
[19] B. Depuydt, G. van Loo, P. Vandenabeele, W. Declercq, Induction of apoptosis by TNF receptor 2 in a T-cell hybridoma is FADD dependent and blocked by caspase-8 inhibitors, J. Cell Sci. 118 (2005) 497–504.
[20] G.T. Baxter, R.C. Kuo, O.J. Jupp, P. Vandenabeele, D.J. MacEwan, Tumor necrosis factor-alpha mediates both apoptotic cell death and cell proliferation in a human hematopoietic cell line dependent on mitotic activity and receptor subtype expression, J. Biol. Chem. 274 (1999) 9539–9547.
[21] W. Declercq, P. Vandenabeele, W. Fiers, Dimerization of chimeric erythropoietin/75 kDa tumour necrosis factor (TNF) receptors transduces TNF signals: necessity for the 75 kDa-TNF receptor transmembrane domain, Cytokine 7 (1995) 701–709.
[22] A.P. Grech, S. Gardam, T. Chan, R. Quinn, R. Gonzales, A. Basten, R. Brink, Tumor necrosis factor receptor 2 (TNFR2) signaling is negatively regulated by a novel, carboxyl-terminal TNFR-associated factor 2 (TRAF2)-binding site, J. Biol. Chem. 280 (2005) 31572–31581.
[23] G. Ruspi, E.M. Schmidt, F. McCann, M. Feldmann, R.O. Williams, A.A. Stoop, J.L. Dean, TNFR2 increases the sensitivity of ligand-induced activation of the p38 MAPK and NF-kappaB pathways and signals TRAF2 protein degradation in macrophages, Cell. Signal. 26 (2014) 683–690.
[24] G.H. Waetzig, P. Rosenstiel, A. Arlt, A. Till, K. Brautigam, H. Schafer, S. Rose-John, D. Seegert, S. Schreiber, Soluble tumor necrosis factor (TNF) receptor-1 induces apoptosis via reverse TNF signaling and autocrine transforming growth factor-beta1, Faseb. J. 19 (2005) 91–93.
[25] T. Gohda, S. Maruyama, N. Kamei, S. Yamaguchi, T. Shibata, M. Murakoshi,

S. Horikoshi, Y. Tomino, I. Ohsawa, H. Gotoh, S. Nojiri, Y. Suzuki, Circulating TNF receptors 1 and 2 predict mortality in patients with end-stage renal disease undergoing dialysis, Sci. Rep. 7 (2017) 43520.
[26] A.C. Carlsson, C.C. Juhlin, T.E. Larsson, A. Larsson, E. Ingelsson, J. Sundstrom, L. Lind, J. Arnlov, Soluble tumor necrosis factor receptor 1 (sTNFR1) is associated with increased total mortality due to cancer and cardiovascular causes - findings from two community based cohorts of elderly, Atherosclerosis 237 (2014) 236–242.
[27] C.I. Park, T. Kurobe, I. Hirono, T. Aoki, Cloning and characterization of cDNAs for two distinct tumor necrosis factor receptor superfamily genes from Japanese flounder Paralichthys olivaceus, Dev. Comp. Immunol. 27 (2003) 365–375.
[28] L. Grayfer, M. Belosevic, Molecular characterization of tumor necrosis factor receptors 1 and 2 of the goldfish (Carassius aurutus L.), Mol. Immunol. 46 (2009) 2190–2199.
[29] S. Zhang, R. Zhang, T. Ma, X. Qiu, X. Wang, A. Zhang, H. Zhou, Identification and functional characterization of tumor necrosis factor receptor 1 (TNFR1) of grass carp (Ctenopharyngodon idella), Fish Shellfish Immunol. 58 (2016) 24–32.
[30] X. Wang, Y. Wang, M. Yang, H. Zhou, A newly identified epithelial cell adhesion molecule (EpCAM) from grass carp (Ctenopharyngodon idellus): cloning, tissue distribution and lipopolysaccharide-induced expression in head kidney leucocytes, Fish Shellfish Immunol. 29 (2010) 998–1002.
[31] L. Du, L. Qin, X. Wang, A. Zhang, H. Wei, H. Zhou, Characterization of grass carp (Ctenopharyngodon idella) IL-17D: molecular cloning, functional implication and signal transduction, Dev. Comp. Immunol. 42 (2014) 220–228.
[32] H. Wei, X. Wang, A. Zhang, L. Du, H. Zhou, Identification of grass carp IL-10 receptor subunits: functional evidence for IL-10 signaling in teleost immunity, Dev. Comp. Immunol. 45 (2014) 259–268.
[33] A. Zhang, D. Chen, H. Wei, L. Du, T. Zhao, X. Wang, H. Zhou, Functional characterization of TNF-alpha in grass carp head kidney leukocytes: induction and involvement in the regulation of NF-kappaB signaling, Fish Shellfish Immunol. 33 (2012) 1123–1132.
[34] X. Yang, S. Wang, L. Du, K. Yang, X. Wang, A. Zhang, H. Zhou, Molecular and functional characterization of IL-1 receptor type 2 in grass carp: a potent inhibitor of IL-1beta signaling in head kidney leukocytes, Dev. Comp. Immunol. 41 (2013) 738–745.
[35] B.B. Aggarwal, S.C. Gupta, J.H. Kim, Historical perspectives on tumor necrosis factor and its superfamily: 25 years later, a golden journey, Blood 119 (2012) 651–665.
[36] J.L. Bodmer, P. Schneider, J. Tschopp, The molecular architecture of the TNF superfamily, Trends Biochem. Sci. 27 (2002) 19–26.
[37] J.H. Naismith, T.Q. Devine, T. Kohno, S.R. Sprang, Structures of the extracellular domain of the type I tumor necrosis factor receptor, Structure 4 (1996) 1251–1262.
[38] P. Vandenabeele, W. Declercq, R. Beyaert, W. Fiers, Two tumour necrosis factor receptors: structure and function, Trends Cell Biol. 5 (1995) 392–399.
[39] P.A. Baeuerle, T. Henkel, Function and activation of NF-kappa B in the immune system, Annu. Rev. Immunol. 12 (1994) 141–179.
[40] Q. Li, I.M. Verma, NF-kappaB regulation in the immune system, Nat. Rev. Immunol. 2 (2002) 725–734.
[41] L.M.O. Caram, R. Ferrari, D.L. Nogueira, M. Oliveira, F.V. Francisqueti, S.E. Tanni, C.R. Correa, I. Godoy, Tumor necrosis factor receptor 2 as a possible marker of COPD in smokers and ex-smokers, Int. J. Chronic Obstr. Pulm. Dis. 12 (2017) 2015–2021.
[42] M. Shimizu, M. Mizuta, M. Usami, N. Inoue, Y. Sakakibara, K. Yamada, M. Konishi, K. Ohta, A. Yachie, Clinical significance of serum soluble TNF receptor II level and soluble TNF receptor II/I ratio as indicators of coronary artery lesion development in Kawasaki disease, Cytokine 108 (2018) 168–172.
[43] S.M. Lee, S. Yang, R.H. Cha, M. Kim, J.N. An, J.H. Paik, D.K. Kim, S.W. Kang, C.S. Lim, Y.S. Kim, J.P. Lee, Circulating TNF receptors are significant prognostic biomarkers for idiopathic membranous nephropathy, PloS One 9 (2014) e104354.
[44] R.A. Black, C.T. Rauch, C.J. Kozlosky, J.J. Peschon, J.L. Slack, M.F. Wolfson, B.J. Castner, K.L. Stocking, P. Reddy, S. Srinivasan, N. Nelson, N. Boiani, K.A. Schooley, M. Gerhart, R. Davis, J.N. Fitzner, R.S. Johnson, R.J. Paxton, C.J. March, D.P. Cerretti, A metalloproteinase disintegrin that releases tumour-necrosis factor-alpha from cells, Nature 385 (1997) 729–733.
[45] M. Feldmann, Development of anti-TNF therapy for rheumatoid arthritis, Nat. Rev. Immunol. 2 (2002) 364–371.
[46] L.M. Sedger, M.F. McDermott, TNF and TNF-receptors: from mediators of cell death and inflammation to therapeutic giants - past, present and future, Cytokine Growth Factor Rev. 25 (2014) 453–472.
[47] X. Cui, L. Chang, Y. Li, Q. Lv, F. Wang, Y. Lin, W. Li, J.D. Meade, J.C. Walden, P. Liang, Trivalent soluble TNF Receptor, a potent TNF-alpha antagonist for the treatment collagen-induced arthritis, Sci. Rep. 8 (2018) 7327.
[48] S.T. Wang, X.Z. Meng, L.S. Li, Y.F. Dang, Y. Fang, Y. Shen, X.Y. Xu, R.Q. Wang, J.L. Li, Biological parameters, immune enzymes, and histological alterations in the livers of grass carp infected with Aeromonas hydrophila, Fish Shellfish Immunol. 70 (2017) 121–128.